



The Destruction and Recreation of the X-Ray Corona in a Changing-look Active Galactic Nucleus

C. Ricci^{1,2,3}, E. Kara⁴, M. Loewenstein^{5,6}, B. Trakhtenbrot⁷, I. Arcavi^{7,8}, R. Remillard⁴, A. C. Fabian⁹, K. C. Gendreau⁵, Z. Arzoumanian⁵, R. Li², L. C. Ho^{2,10}, C. L. MacLeod¹¹, E. Cackett¹², D. Altamirano¹³, P. Gandhi¹³, P. Kosec⁹, D. Pasham⁴, J. Steiner⁴, and C.-H. Chan^{7,14}

¹ Núcleo de Astronomía de la Facultad de Ingeniería, Universidad Diego Portales, Av. Ejército Libertador 441, Santiago, Chile; claudio.ricci@mail.udp.cl

² Kavli Institute for Astronomy and Astrophysics, Peking University, Beijing 100871, People's Republic of China

³ George Mason University, Department of Physics & Astronomy, MS 3F3, 4400 University Drive, Fairfax, VA 22030, USA

⁴ MIT Kavli Institute for Astrophysics and Space Research, 70 Vassar Street, Cambridge, MA 02139, USA

⁵ Astrophysics Science Division, NASA Goddard Space Flight Center, 8800 Greenbelt Road, Greenbelt, MD 20771, USA

⁶ Department of Astronomy, University of Maryland, College Park, MD 20742, USA

⁷ School of Physics and Astronomy, Tel Aviv University, Tel Aviv 69978, Israel

⁸ CIFAR Azrieli Global Scholars program, CIFAR, Toronto, Canada

⁹ Institute of Astronomy, University of Cambridge, Madingley Road, CB3 0HA Cambridge, UK

¹⁰ Department of Astronomy, School of Physics, Peking University, Beijing 100871, People's Republic of China

¹¹ Center for Astrophysics, Harvard & Smithsonian, 60 Garden Street, Cambridge, MA 02138-1516, USA

¹² Department of Physics & Astronomy, Wayne State University, 666 West Hancock Street, Detroit, MI 48201, USA

¹³ Department of Physics & Astronomy, University of Southampton, Southampton, Hampshire SO17 1BJ, UK

¹⁴ Racah Institute of Physics, Hebrew University of Jerusalem, Jerusalem 91904, Israel

Received 2020 April 22; revised 2020 May 6; accepted 2020 May 8; published 2020 July 16

Abstract

We present the drastic transformation of the X-ray properties of the active galactic nucleus (AGN) 1ES 1927+654, following a changing-look event. After the optical/ultraviolet outburst the power-law component, produced in the X-ray corona, disappeared, and the spectrum of 1ES 1927+65 instead became dominated by a blackbody component ($kT \sim 80\text{--}120$ eV). This implies that the X-ray corona, ubiquitously found in AGNs, was destroyed in the event. Our dense ~ 450 days long X-ray monitoring shows that the source is extremely variable in the X-ray band. On long timescales the source varies up to ~ 4 dex in ~ 100 days, while on short timescales up to ~ 2 dex in ~ 8 hr. The luminosity of the source is found to first show a strong dip down to $\sim 10^{40}$ erg s⁻¹, and then a constant increase in luminosity to levels exceeding the pre-outburst level $\gtrsim 300$ days after the optical event detection, rising up asymptotically to $\sim 2 \times 10^{44}$ erg s⁻¹. As the X-ray luminosity of the source increases, the X-ray corona is recreated, and a very steep power-law component ($\Gamma \simeq 3$) reappears, and dominates the emission for 0.3–2 keV luminosities $\gtrsim 10^{43.7}$ erg s⁻¹, ~ 300 days after the beginning of the event. We discuss possible origins of this event, and speculate that our observations could be explained by the interaction between the accretion flow and debris from a tidally disrupted star. Our results show that changing-look events can be associated with dramatic and rapid transformations of the innermost regions of accreting supermassive black holes.

Unified Astronomy Thesaurus concepts: Active galactic nuclei (16); Active galaxies (17); High energy astrophysics (739); X-ray active galactic nuclei (2035); Quasars (1319); X-ray quasars (1821); Supermassive black holes (1663)

1. Introduction

Accreting supermassive black holes (SMBHs) are known to show variable optical, ultraviolet (UV), and X-ray emission. One of the most intriguing aspects of this behavior is associated with “changing-look” sources, in which the optical/UV broad emission lines, produced by rapidly moving material surrounding the SMBH (e.g., Kaspi et al. 2000), appear or disappear (e.g., Shappee et al. 2014; LaMassa et al. 2015; Trakhtenbrot et al. 2019). This implies that changing-look active galactic nuclei (AGNs) transition from type 1 (showing both broad and narrow ionic emission lines in the optical) to type 2 (showing only narrow lines), or vice versa. The physical mechanism producing these changing-look events is still hotly debated; the observed changes could be related to radiation pressure instabilities in the disk (Śniegowska & Czerny 2019), to state transitions (Noda & Done 2018; Ruan et al. 2019), or to variations in accretion rate (Elitzur et al. 2014), possibly related to transient events (Merloni et al. 2015), with the source going through a highly accreting phase and producing broad lines.

So far only a few dozens of these systems have been discovered (e.g., Yang et al. 2018; MacLeod et al. 2019) and, due to their rarity, it has been very difficult to catch any of them during the transition phase. We were recently able to observe, for the first time, an AGN in the act of changing phase. 1ES 1927+654 ($z = 0.019422$; Trakhtenbrot et al. 2019) was previously classified as a type 2 AGN (e.g., Gallo et al. 2013 and references therein). In March 2018 the All-Sky Automated Survey for SuperNovae (Shappee et al. 2014) showed that the source suddenly increased in flux by an order of magnitude in the optical V-band (ASASSN-18el/AT2018zf, Nicholls et al. 2018). The analysis of Asteroid Terrestrial-impact Last Alert System (ATLAS; Tonry et al. 2018) data indicated that the event was first detected on 2017 December 23. An optical spectroscopic follow-up campaign showed first a very blue continuum and then, 1–3 months after the optical flux rise, evidence of strong broad Balmer emission lines (Trakhtenbrot et al. 2019).

Right after the appearance of the broad optical lines we started monitoring the source in the X-ray band. X-rays in

AGNs are primarily created by Comptonization of optical/UV disk photons in a corona of hot electrons, located within a light-hour from the accreting system (Fabian et al. 2009), and likely powered by the magnetic field of the accretion disk (Merloni & Fabian 2001). These electrons transfer their energy to the disk photons, up-scattering them into the X-rays (Haardt & Maraschi 1991), and creating the power-law continuum ubiquitously found in AGNs. X-ray observations therefore provide an extremely powerful tool to study the inner regions of AGNs and the physical conditions of the accretion flow. In this work we discuss the peculiar X-ray properties of 1ES 1927+654 after the changing-look event. Throughout the Letter we adopt standard cosmological parameters ($H_0 = 70 \text{ km s}^{-1} \text{ Mpc}^{-1}$, $\Omega_m = 0.3$, $\Omega_\Lambda = 0.7$). Unless otherwise stated, uncertainties are quoted at the 90% confidence level.

2. The Disappearance and Reappearance of the Power-law Component

Our X-ray campaign consists of 265 Neutron star Interior Composition Explorer (NICER; Gendreau et al. 2012; Arzoumanian et al. 2014) observations (for a total of 678ks), 14 Neil Gehrels Swift Observatory (Gehrels et al. 2004) observations (26 ks), and three joint X-ray Multi-Mirror Mission (XMM)-Newton/Nuclear Spectroscopic Telescope Array (NuSTAR; Jansen et al. 2001; Harrison et al. 2013) observations (158/169 ks). Details about the data reduction and spectral analysis of all these X-ray observations are reported in a dedicated companion publication (Ricci et al. 2020, see also Kara et al. 2018), while here we focus on the unexpected spectral properties of 1ES 1927+654 after the changing-look event.

Our monitoring campaign shows that the source is extremely variable in the 0.5–10 keV band (panel (A) of Figure 1), with very strong intraday variability (up to ~ 2 dex in ~ 8 hr). However, the strongest variability is found on longer time-scales. The first X-ray observations, carried out in 2018 May, found 1ES 1927+654 at a similar luminosity level of the previous XMM-Newton observation ($L_{0.5-10} = 8.3 \times 10^{42} \text{ erg s}^{-1}$, Gallo et al. 2013; green dotted-dashed line in panel (A) of Figure 1). At $t \sim 160$ days from the optical event detection the luminosity of the source started to decrease rapidly, reaching $L_{0.5-10} \sim 10^{40} \text{ erg s}^{-1}$ at $t \sim 200$ days. After this dip we observed a constant increase in luminosity, to levels exceeding the pre-outburst value at $t \gtrsim 300$ days. The luminosity then rose up asymptotically to $\sim 2 \times 10^{44} \text{ erg s}^{-1}$, with the intraday variability decreasing to ~ 0.4 dex. The X-ray flux variability is tightly connected with the spectral variability, with the source showing a clear harder-when-brighter behavior (panels (B) and (C) of Figure 1). Interestingly, the X-ray and optical/UV fluxes are completely disconnected, with the latter showing a monotonic declining trend for $t > 150$ days (Panel (D) and Trakhtenbrot et al. 2019).

Previous X-ray observations (Gallo et al. 2013) of 1ES 1927+654 (gray spectrum in Figure 2) found that the source is unobscured ($N_H \simeq 10^{20} \text{ cm}^{-2}$), and that its X-ray spectrum could be well represented by a model that includes a power-law ($\Gamma = 2.39 \pm 0.04$) and a blackbody component ($kT = 170 \pm 5 \text{ eV}$). After the optical brightening event, 1ES 1927+654 showed a spectrum completely different from the 2011 XMM-Newton observation.

observation of our campaign (2018 June, red spectrum in Figure 2), the spectrum was extremely soft, with the emission being dominated by a blackbody-like component. The disappearance of the power-law component, which has not hitherto been observed in AGNs, implies that the dramatic event that created the broad lines also destroyed the X-ray corona. The X-ray spectra of 1ES 1927+654 can be typically well modeled by a blackbody, two Gaussian emission lines and a power-law component. Absorption from outflowing ionized gas (with $N_H \sim 10^{20} \text{ cm}^{-2}$) is also clearly observed in the XMM-Newton/Reflection Grating Spectrometer (RGS) observations (see Ricci et al. 2020). During the 2018 June XMM-Newton observation the blackbody was found to have a temperature of $kT = 102 \pm 1 \text{ eV}$, and only a very faint power-law emission was detected at $E \gtrsim 1.5 \text{ keV}$, carrying a very small fraction ($0.4 \pm 0.3\%$) of the total 0.3–2 keV flux. The power-law component is undetected or extremely faint also in the observations carried out by NICER in 2018 July, when the luminosity was at its lowest level, and in 2018 August (spectra 2 and 3 in Figure 2, respectively). The spectral analysis of the stacked NICER spectra, obtained combining observations carried out in June to 2018 mid-August, recovered only upper limits for the ratio between the power-law and blackbody flux in the 0.3–2 keV band. These upper limits range between $\lesssim 0.5\%$ (2018 June) and $\lesssim 6\%$ (2018 August). As the luminosity of the source increased above the pre-outburst level, our XMM-Newton/NuSTAR and NICER observations show that the power-law component reappeared (spectra 4 and 5). Interestingly, the photon index of this power-law component, $\Gamma \simeq 3$, is considerably higher than what is commonly found in AGNs ($\Gamma \sim 1.8$; e.g., Ricci et al. 2017).

In the X-ray observations carried out in late 2018 and in 2019 the fraction of the total 0.3–2 keV flux ascribed to the power-law component is significantly higher than in June–August 2018, and is found to dominate the X-ray emission in the May 2019 ($F_{\text{pow}}/F_{\text{bb}} = 1.45^{+0.13}_{-0.16}$) XMM-Newton/NuSTAR observation. An increase with the luminosity of the ratio between the flux of the power law and that of the blackbody is clearly detected when stacking the NICER observations based on their 0.5–10 keV luminosities (cyan stars in Figure 3). At the lowest luminosities ($L_{0.5-10} \sim 10^{40} - 10^{41} \text{ erg s}^{-1}$) the ratio is $F_{\text{pow}}/F_{\text{bb}} \leq 0.003$, which is $\gtrsim 850$ times lower than the value found in 2011 ($F_{\text{pow}}/F_{\text{bb}} = 2.6 \pm 0.2$), before the optical outburst. The power law starts to dominate over the blackbody component for 0.3–2 keV luminosities $\gtrsim 10^{43.7} \text{ erg s}^{-1}$, reaching a ratio between the power law and the blackbody flux similar to that found in the 2011 observations at $\sim 10^{44} \text{ erg s}^{-1}$. All this shows that, as the source becomes brighter, the X-ray corona is being recreated. Such a transition has not been observed before. This can also be observed by comparing the light curve to a model-independent flux ratio and to $F_{\text{pow}}/F_{\text{bb}}$ (panels (B) and (C) of Figure 1). Our spectral analysis of the two latest XMM-Newton/NuSTAR observations, which display a strong power-law component, shows that a cutoff at $E_C \simeq 3 \text{ keV}$ is needed to reproduce the data (see Ricci et al. 2020 for details). This cutoff energy is considerably lower than that observed in AGNs ($E_C \sim 50 - 300 \text{ keV}$; e.g., Ricci et al. 2017), and points to a temperature of the corona of just $kT_e \simeq 1.5 \text{ keV}$, assuming that the Comptonizing plasma is optically thin. This assumption is supported by the fact that, considering Γ and E_C , and using Equation (6) of Ricci et al. (2018), the optical depth of the plasma would be $\tau \sim 0.15$. The

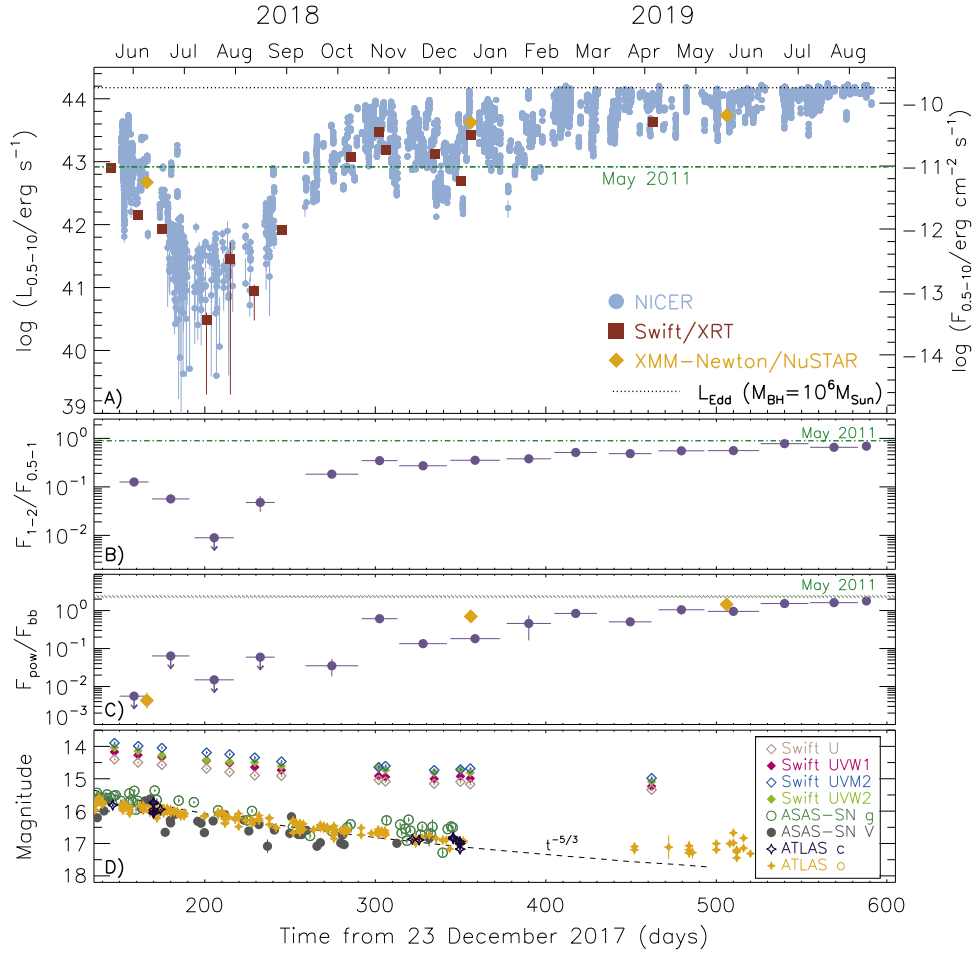


Figure 1. Long-term light curve of 1ES 1927+654. Panel (A): 0.5–10 keV light curve, including NICER (cyan circles), Swift/X-Ray Telescope (XRT; red squares) and XMM-Newton/NuSTAR (yellow diamonds) data. Our first X-ray observation (2018 May 17) was carried out ~ 150 days after the detection of the outburst in the optical (2017 December 23; Trakhtenbrot et al. 2019). The 0.5–10 keV luminosity before the event, inferred by the 2011 XMM-Newton observation (Gallo et al. 2013), was 8.3×10^{42} erg s $^{-1}$ (horizontal green dotted–dashed line). The black dotted line represents the possible Eddington luminosity for $M_{\text{BH}} = 10^6 M_{\odot}$ (see the Appendix). Panel (B): ratio between the 1–2 keV and 0.5–1 keV flux for the NICER observations, showing the softening after the event, followed by an hardening as the overall luminosity increased. Panel (C): ratio between the power-law and blackbody flux in the 0.5–2 keV band. Panel (D): optical/UV light curve (Trakhtenbrot et al. 2019), showing a very different behavior with respect to the X-ray band. The time of the event (t_0) adopted for the $t^{-5/3}$ curve (black dashed line) is 2017 December 23.

low temperature and optical depth also suggest that the X-ray corona is in the process of being reformed, and could imply that the magnetic field powering it is still not strong enough to support the typical X-ray emitting plasma found in AGNs.

3. Discussion

The surprisingly soft X-ray continuum (Figure 2), together with the dramatic X-ray variability (Figure 1), suggests that the source underwent some catastrophic event that restructured its accretion flow. The lack of X-ray flux above 2 keV implies that the event strongly affected the X-ray corona (and possibly the innermost regions of the accretion flow), possibly completely destroying it. As the X-ray luminosity of 1ES 1927+654 increases, the power-law component reappears, and starts to dominate the overall 0.3–2 keV flux (Figure 3). This suggests that the X-ray corona is in the process of being recreated.

It has been argued that changing-look events in AGN might be powered by hard-to-soft state transitions (Noda & Done 2018; Ruan et al. 2019), analogous to those observed in black hole X-ray binaries, where the inner disk evaporates into an advection-dominated accretion flow. In this scenario the

timescales for the evaporation of the accretion flow should be the viscous timescale. The very soft spectrum of 1ES 1927+654 is reminiscent of the spectral shape of black hole X-ray binaries in the high/soft state (e.g., Remillard & McClintock 2006), and the asymptotic behavior of the luminosity is similar to Eddington-limited accretion outbursts observed in stellar-mass systems (e.g., Kimura et al. 2016). However, the timescales expected for a state transition (e.g., Dunn et al. 2010) of a $10^6 M_{\odot}$ black hole are considerably longer (~ 100 yr) than what we observe in 1ES 1927+654, where the spectral variations happen on timescales of hours. Strong magnetization (Noda & Done 2018), possibly coupled with geometrically thick disks (Dexter & Begelman 2019), could reduce the timescales, but would not be able to explain the spectral variability on $\lesssim 1$ day intervals detected by our NICER and XMM-Newton observations.

The event that destroyed the X-ray corona, while increasing the optical/UV flux and creating the broad Balmer lines, could be related to the tidal disruption of a star by the SMBH. While tidal disruption events (TDEs) are rare (e.g., Kawamuro et al. 2016), it has been argued that the presence of a long-lived accretion disk can enhance their rate with respect to inactive

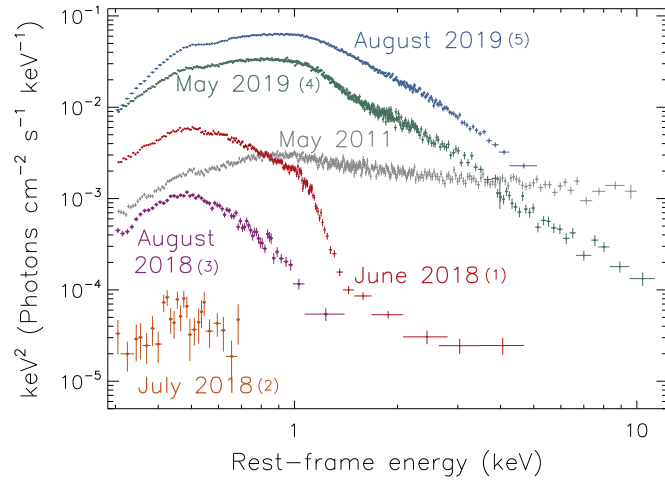


Figure 2. X-ray spectral evolution of IES 1927+654. Spectra of the 2011 May (gray points; XMM-Newton European Photon Imaging Camera (EPIC)/PN), 2018 June (red points; XMM-Newton EPIC/PN and Metal Oxide Semiconductor (MOS)), 2018 July (orange points; NICER), 2018 August (purple points; NICER), May 2019 (green points; XMM-Newton EPIC/PN and NuSTAR) and 2019 July (blue points; NICER) observations. Soon after the event (2018 June–August) the X-ray spectrum of IES 1927+654 was extremely soft, and did not show the strong hard X-ray component ubiquitously found in AGN and present during the 2011 observation. In the observations carried out in 2019 the flux of the source is higher and a steep power-law component has reappeared.

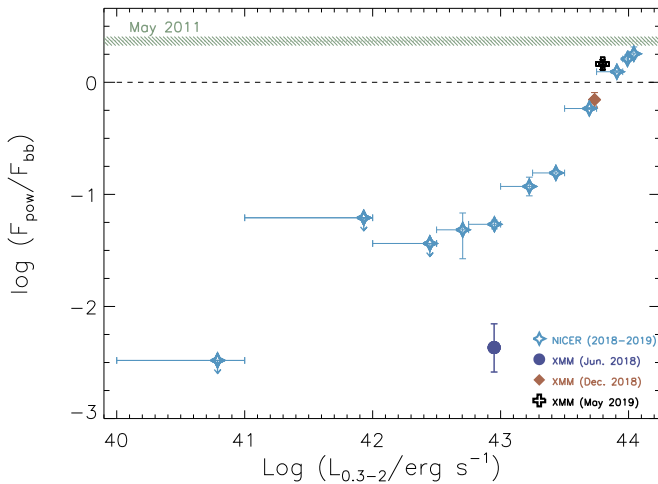


Figure 3. Ratio between the flux of the power-law (F_{pow}) and blackbody (F_{bb}) component vs. the 0.3–2 keV luminosity for the NICER (2018 May to 2019 August) and XMM-Newton observations. The horizontal black dashed line represents the $F_{\text{pow}} = F_{\text{bb}}$ case. The plot shows a clear positive relation between $F_{\text{pow}}/F_{\text{bb}}$ and the luminosity, with the spectrum becoming dominated by the power-law emission at $\log(L_{0.3-2}/\text{erg s}^{-1}) \approx 43.7$, and reaching the level of $F_{\text{pow}}/F_{\text{bb}}$ observed in 2011 (green squares) at $\approx 10^{44} \text{ erg s}^{-1}$.

galaxies (e.g., Karas & Šubr 2007). TDEs have been discussed as a possible driver of changing-look events (Merloni et al. 2015), and a few cases of AGN in which a TDE might have occurred have been reported over the past few years (e.g., Liu et al. 2020). Merloni et al. (2015) found that the changing-look AGN SDSS 0159 + 003 (LaMassa et al. 2015) displays a $t^{-5/3}$ behavior, which is typical of TDEs (Rees 1988), and argued that the event could be related to the disruption of a star by a $\sim 10^8 M_{\odot}$ SMBH. Campana et al. (2015) discussed how the strong variability of IC 3599 could be explained by multiple TDE events recurring every 9.5 yr. Blanchard et al. (2017) proposed that the transient PS16dtm was due a TDE in a pre-

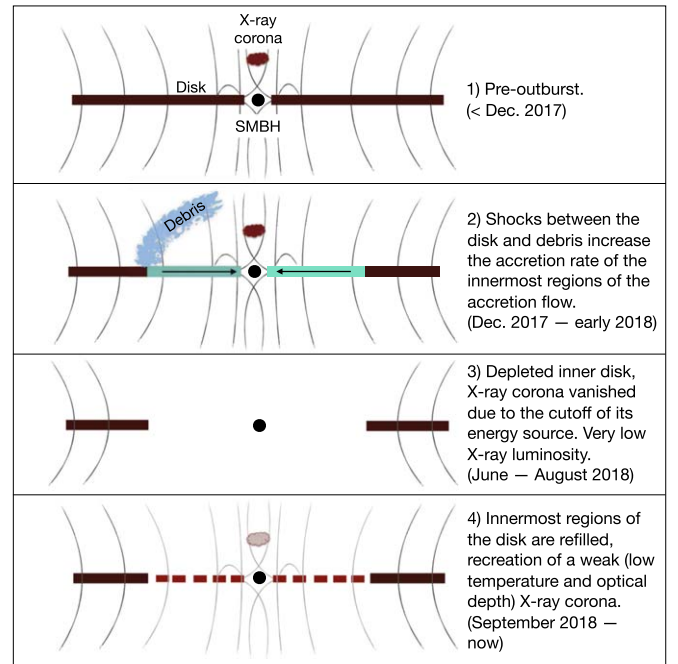


Figure 4. Schematic representation of the TDE scenario. The innermost regions of the accretion disk, where the magnetic field (black lines) powers the X-ray corona (1), are strongly affected by the interaction with the debris (2). The shocks excited by the debris increase the accretion rate in the inner disk, leading to a depletion of the accretion flow (3). Due to the disappearance of the inner disk and of its magnetic field, the X-ray corona is destroyed. As the disk is replenished the magnetic field starts reforming, together with the X-ray corona (4).

existing narrow-line Seyfert 1 AGN with a $\sim 10^6 M_{\odot}$ black hole. In this source the increase in the UV and optical flux was not accompanied by an increase of the X-ray flux, which was found to be at least an order of magnitude below the previous XMM-Newton detection. Blanchard et al. (2017) argued that this might be due to absorption of the X-ray corona caused by the disk of debris.

The very soft X-ray emission observed after the event, and the fact that the optical/UV flux decreases following a trend consistent with the $t^{-5/3}$ behavior (Trakhtenbrot et al. 2019), are in agreement with the TDE scenario (e.g., Komossa 2015; Auchettl et al. 2017), while the re-brightening observed in the X-rays is very different from what is typically observed in TDEs. Interestingly, the behavior seen in IES 1927+654 might be consistent with recent hydrodynamic simulations of a debris stream colliding with an accretion disk (Chan et al. 2019). In this scenario, schematically illustrated in Figure 4, the innermost regions of the accretion flow, where the X-ray coronal power-law component is produced, accrete faster than the outer parts, due to the efficient removal of angular momentum by shocks excited in the disk by the debris. The enhanced accretion rate empties the inner disk, which would lead to the destruction of the magnetic field pattern and cutting off the energy source of the X-ray corona. The disruption of the corona leads to the disappearance of the power-law component and to a drastic decrease of the X-ray luminosity of the system. The non-steady accretion flow and/or the shocks could be responsible for the soft component observed below 2 keV (see also Ricci et al. 2020). The lack of UV broad lines (Trakhtenbrot et al. 2019) with ionization energy $\chi_{\text{ion}} \gtrsim 15 \text{ eV}$, such as Mg II $\lambda 2798$ ($\chi_{\text{ion}} = 15.04 \text{ eV}$) and C IV $\lambda 1549$ ($\chi_{\text{ion}} = 64.49 \text{ eV}$), also suggests a depletion of the inner disk.

As the inner disk is replenished by material flowing in from the outer disk, the magnetic field around the SMBH is reformed, and restarts powering the X-ray corona; this leads to the reappearance of the power-law component in the X-ray spectrum. During this period an increase in the overall X-ray luminosity is expected, consistent with our observations. The asymptotic luminosity limit at $\sim 1.5 \times 10^{44} \text{ erg s}^{-1}$ might indicate that, in this framework, the replenishment of the disk is Eddington-limited (Figure 2). Interestingly, the observed decrease of the X-ray flux in PS16dtm after the event is similar to what we found for IES 1927+654 during the first months after the event, although no re-brightening has been observed so far in this source. IES 1927+654 also shares some observational properties with super-soft AGN (e.g., Terashima et al. 2012; Miniutti et al. 2019; Giustini et al. 2020), objects that could be associated to TDEs (e.g., Shu et al. 2018; King 2020), such as the harder-when-brighter behavior (see Ricci et al. 2020 for details), and a very prominent blackbody component, in particular during the lower luminosity intervals.

4. Summary and Conclusions

IES 1927+654 is a type 2 AGN that was recently found to develop broad optical emission lines after an optical outburst (2017 December 23; Trakhtenbrot et al. 2019). Following the changing-look event, we started an intense 450 days X-ray monitoring campaign, which includes observations from NICER (265 pointings), Swift (14), and XMM-Newton/NuSTAR (3). Our observations show the following.

1. The source is extremely variable both on long and short timescales (see Figure 1), with the flux changing up to ~ 4 dex in ~ 100 days, and up to ~ 2 dex in ~ 8 hr. The luminosity of the source is found to first show a strong dip down to $\sim 10^{40} \text{ erg s}^{-1}$, and then a constant increase in luminosity to levels exceeding the pre-outburst level $\gtrsim 300$ days after the optical event detection, rising up asymptotically to $\sim 2 \times 10^{44} \text{ erg s}^{-1}$.
2. After the optical outburst the power-law component produced in the X-ray corona, which is ubiquitously observed in AGNs, was found to have almost completely disappeared (Figure 2). The X-ray spectrum was instead dominated by a very strong blackbody component with $kT \simeq 100 \text{ eV}$. During the first (2018 May–August) observations only a very faint power-law emission was detected at $E \gtrsim 1.5 \text{ keV}$, carrying only $\lesssim 1\%$ of the total 0.3–2 keV flux.
3. A clear positive correlation between the ratio of the power-law and blackbody flux ($F_{\text{pow}}/F_{\text{bb}}$) in the 0.3–2 keV range and the luminosity is found stacking the NICER spectra (Figure 3). At the lowest luminosities ($L_{0.5-10} \sim 10^{40} - 10^{41} \text{ erg s}^{-1}$) the ratio is $F_{\text{pow}}/F_{\text{bb}} \leq 0.003$, i.e., $\gtrsim 850$ times lower than the value found in 2011 ($F_{\text{pow}}/F_{\text{bb}} = 2.6 \pm 0.2$), before the optical outburst. As the X-ray luminosity of the source increases, the X-ray corona is recreated, and a very soft power-law component ($\Gamma \simeq 3$) reappears, and dominates the emission for 0.3–2 keV luminosities $\gtrsim 10^{43.7} \text{ erg s}^{-1}$, ~ 300 days after the beginning of the event.

These results show that changing-look events can be associated with dramatic and rapid transformations of the innermost regions of accreting SMBHs. We speculate that the behavior of IES 1927+654 could be caused by the tidal

disruption of a star by the accreting black hole, which is expected to deplete the innermost regions of the accretion flow (Chan et al. 2019), therefore disrupting the magnetic field powering the X-ray corona (Figure 4). As the inner regions of the accretion flows are replenished, the magnetic field around the SMBH is reformed, and restarts powering the X-ray corona. This would lead to the reappearance of the power-law component and to the increase of the X-ray luminosity.

Our coordinated multi-wavelength observations of the dramatic transformation of IES 1927+654 offer an unprecedented opportunity to probe accretion physics, and to understand the relation between changing-look events and the innermost regions of the accreting system. Upcoming surveys, such as those that are or will be carried out by eROSITA (Merloni et al. 2012), the Einstein Probe (Yuan et al. 2015), and SDSS-V (Kollmeier et al. 2017), are designed to reveal large samples of similar events, allowing to further constrain the typical timescales and the occurrence rates of such transformative events, and to understand their importance to massive black hole growth.

We thank the referee for their comments, which helped us improve the quality of the manuscript. We acknowledge XMM-Newton, NuSTAR, and Swift for the DDT observations they kindly guaranteed us. L.H. acknowledges financial support from the National Key R&D Program of China grant No. 2016YFA0400702, and the National Science Foundation of China grants No. 11473002 and 1721303. C.R. acknowledges support from the Fondecyt Iniciacion grant 11190831. I.A. is a CIFAR Azrieli Global Scholar in the Gravity and the Extreme Universe Program and acknowledges support from that program, from the Israel Science Foundation (grant No. 2108/18 and 2752/19), from the United States–Israel Binational Science Foundation (BSF), and from the Israeli Council for Higher Education Alon Fellowship. P.G. acknowledges support from STFC and a UGC-UKIERI Thematic Partnership. D.A. acknowledges support from the Royal Society. C.H.C. is supported by ERC advanced grant “TRex” and the CHE-ISF Center for Excellence in Astrophysics. B.T. acknowledges support from the Israel Science Foundation (grant No. 1849/19). C.R. acknowledges F. Bauer, C.S. Chang, and the Santiago AGN community for useful discussion. Based on observations with the NASA/ESA/CSA Hubble Space Telescope obtained [from the Data Archive] at the Space Telescope Science Institute, which is operated by the Association of Universities for Research in Astronomy, Incorporated, under NASA contract NAS5-26555. Support for Cycle 25 Program GO-15604 was provided through a grant from the STScI under NASA contract NAS5-26555.

Facilities: NICER, Swift, XMM-Newton, NuSTAR.

Appendix Black Hole Mass and Eddington Ratio

A black hole mass of $1.9 \times 10^7 M_{\odot}$ has been inferred by considering the width of the broad Balmer lines (Trakhtenbrot et al. 2019). However, due to the transient nature of the event, the clouds emitting the broad Balmer lines might not have had the time to virialize, as shown by their variable widths (Trakhtenbrot et al. 2019). The stellar mass of the galaxy inferred from *K*-band photometry (e.g., Kormendy & Ho 2013) suggests a lower black hole mass ($M_{\text{BH}} \sim 10^6 M_{\odot}$; R. Li et al. 2020, in preparation).

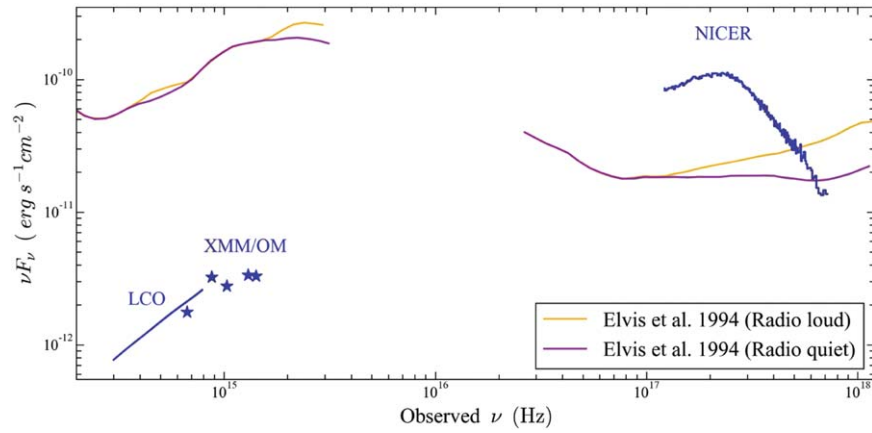


Figure A1. Spectral energy distribution of 1ES 1927+654 at late times ($t \gtrsim 450$). The figure illustrates the NICER (2019 August 3, ID: 2200190277), XMM-Newton/OM (2019 May 6, ID: 0843270101), and Las Cumbres Observatory (2019 July 25) observations of 1ES 1927+654, together with the typical spectral energy distribution of radio-quiet and radio-loud AGNs (Elvis et al. 1994). The host galaxy emission was subtracted from the optical/UV data (R. Li et al. 2020, in preparation).

At times $\gtrsim 300$ days after the event the optical/UV flux had decreased strongly (Trakhtenbrot et al. 2019; panel (D) of Figure 1), and most of the emission could be produced in the X-rays. The variability in the X-rays and optical/UV are in fact completely uncorrelated (Figure 1) and a very strong emission in the X-ray band does not correspond to an increased flux in the optical/UV. While the X-ray emission oscillates between $\sim 10^{43}$ erg s $^{-1}$ and $\sim 2 \times 10^{44}$ erg s $^{-1}$, the bolometric luminosity inferred from the 5100 Å flux (using a bolometric correction of $\kappa_{\text{bol}} = 9$; Kaspi et al. 2000) is considerably lower ($\sim 5 \times 10^{42}$ erg s $^{-1}$). Similarly, even considering the bolometric luminosity from the near-UV ($\kappa_{\text{bol}} = 2\text{--}4$; Trakhtenbrot & Netzer 2012) one would obtain $\sim (1 - 3) \times 10^{43}$ erg s $^{-1}$. Thus, at the highest X-ray luminosities, the 0.5–10 keV emission is $\sim 1\text{--}2$ orders of magnitude higher than the bolometric luminosity inferred from the optical or UV. This is also illustrated in Figure A1, which shows that the spectral energy distribution of the source appears to be dominated by the X-ray emission, and is very different from what is typically found in AGNs (Elvis et al. 1994). Therefore at $L_{0.5-10} \simeq 10^{44}$ erg s $^{-1}$ we could consider a 0.5–10 keV bolometric correction of ~ 1 , and the maximum luminosity of 1ES 1927+654 would correspond to $\lambda_{\text{Edd}} \sim 1$ for $M_{\text{BH}} \sim 10^6 M_{\odot}$ (see panel (A) of Figure 1).

ORCID iDs

C. Ricci <https://orcid.org/0000-0001-5231-2645>
 E. Kara <https://orcid.org/0000-0003-0172-0854>
 B. Trakhtenbrot <https://orcid.org/0000-0002-3683-7297>
 I. Arcavi <https://orcid.org/0000-0001-7090-4898>
 R. Remillard <https://orcid.org/0000-0003-4815-0481>
 A. C. Fabian <https://orcid.org/0000-0002-9378-4072>
 L. C. Ho <https://orcid.org/0000-0001-6947-5846>
 E. Cackett <https://orcid.org/0000-0002-8294-9281>
 D. Altamirano <https://orcid.org/0000-0002-3422-0074>
 P. Gandhi <https://orcid.org/0000-0003-3105-2615>
 J. Steiner <https://orcid.org/0000-0002-5872-6061>
 C.-H. Chan <https://orcid.org/0000-0001-5949-6109>

References

Arzoumanian, Z., Gendreau, K. C., Baker, C. L., et al. 2014, *Proc. SPIE*, 9144, 914420

- Auchettl, K., Guillochon, J., & Ramirez-Ruiz, E. 2017, *ApJ*, 838, 149
 Blanchard, P. K., Nicholl, M., Berger, E., et al. 2017, *ApJ*, 843, 106
 Campana, S., Mainetti, D., Colpi, M., et al. 2015, *A&A*, 581, A17
 Chan, C.-H., Piran, T., Krolik, J. H., & Saban, D. 2019, *ApJ*, 881, 113
 Dexter, J., & Begelman, M. C. 2019, *MNRAS*, 483, L17
 Dunn, R. J. H., Fender, R. P., Körding, E. G., Belloni, T., & Cabanac, C. 2010, *MNRAS*, 403, 61
 Elitzur, M., Ho, L. C., & Trump, J. R. 2014, *MNRAS*, 438, 3340
 Elvis, M., Wilkes, B. J., McDowell, J. C., et al. 1994, *ApJS*, 95, 1
 Fabian, A. C., Zoghbi, A., Ross, R. R., et al. 2009, *Natur*, 459, 540
 Gallo, L. C., MacMackin, C., Vasudevan, R., et al. 2013, *MNRAS*, 433, 421
 Gehrels, N., Chincarini, G., Giommi, P., et al. 2004, *ApJ*, 611, 1005
 Gendreau, K. C., Arzoumanian, Z., & Okajima, T. 2012, *Proc. SPIE*, 8443, 844313
 Giustini, M., Miniutti, G., & Saxton, R. D. 2020, *A&A*, 636, L2
 Haardt, F., & Maraschi, L. 1991, *ApJ*, 380, L51
 Harrison, F. A., Craig, W. W., Christensen, F. E., et al. 2013, *ApJ*, 770, 103
 Jansen, F., Lumb, D., Altieri, B., et al. 2001, *A&A*, 365, L1
 Kara, E., Loewenstein, M., Remillard, R. A., et al. 2018, *ATel*, 12169
 Karas, V., & Šubr, L. 2007, *A&A*, 470, 11
 Kaspi, S., Smith, P. S., Netzer, H., et al. 2000, *ApJ*, 533, 631
 Kawamuro, T., Ueda, Y., Shidatsu, M., et al. 2016, *PASJ*, 68, 58
 Kimura, M., Isogai, K., Kato, T., et al. 2016, *Natur*, 529, 54
 King, A. 2020, *MNRAS*, 493, L120
 Kollmeier, J. A., Zasowski, G., Rix, H.-W., et al. 2017, arXiv:1711.03234
 Komossa, S. 2015, *JHEAp*, 7, 148
 Kormendy, J., & Ho, L. C. 2013, *ARA&A*, 51, 511
 LaMassa, S. M., Cales, S., Moran, E. C., et al. 2015, *ApJ*, 800, 144
 Liu, Z., Li, D., Liu, H.-Y., et al. 2020, *ApJ*, 894, 93
 MacLeod, C. L., Green, P. J., Anderson, S. F., et al. 2019, *ApJ*, 874, 8
 Merloni, A., Dwelly, T., Salvato, M., et al. 2015, *MNRAS*, 452, 69
 Merloni, A., & Fabian, A. C. 2001, *MNRAS*, 321, 549
 Merloni, A., Predehl, P., Becker, W., et al. 2012, arXiv:1209.3114
 Miniutti, G., Saxton, R. D., Giustini, M., et al. 2019, *Natur*, 573, 381
 Nicholls, B., Brimacombe, J., Kiyota, S., et al. 2018, *ATel*, 11391
 Noda, H., & Done, C. 2018, *MNRAS*, 480, 3898
 Rees, M. J. 1988, *Natur*, 333, 523
 Remillard, R. A., & McClintock, J. E. 2006, *ARA&A*, 44, 49
 Ricci, C., Ho, L. C., Fabian, A. C., et al. 2018, *MNRAS*, 480, 1819
 Ricci, C., Trakhtenbrot, B., Koss, M. J., et al. 2017, *ApJS*, 233, 17
 Ricci, C., et al. 2020, *ApJ*, submitted
 Ruan, J. J., Anderson, S. F., Eracleous, M., et al. 2019, *ApJ*, 883, 76
 Shappee, B. J., Prieto, J. L., Grupe, D., et al. 2014, *ApJ*, 788, 48
 Shu, X. W., Wang, S. S., Dou, L. M., et al. 2018, *ApJ*, 857, L16
 Śniegowska, M., & Czerny, B. 2019, arXiv:1904.06767
 Terashima, Y., Kamizasa, N., Awaki, H., Kubota, A., & Ueda, Y. 2012, *ApJ*, 752, 154
 Tonry, J. L., Denneau, L., Heinze, A. N., et al. 2018, *PASP*, 130, 064505
 Trakhtenbrot, B., Arcavi, I., MacLeod, C. L., et al. 2019, *ApJ*, 883, 94
 Trakhtenbrot, B., & Netzer, H. 2012, *MNRAS*, 427, 3081
 Yang, Q., Wu, X.-B., Fan, X., et al. 2018, *ApJ*, 862, 109
 Yuan, W., Zhang, C., Feng, H., et al. 2015, arXiv:1506.07735